Applied Catalysis A: General 372 (2010) 167–174

Contents lists available at ScienceDirect

Applied Catalysis A: General

journal homepage: www.elsevier.com/locate/apcata

Catalytic oxidative cracking of hexane as a route to olefins

Cassia Boyadjian, Leon Lefferts *, K. Seshan

Catalytic Processes & Materials, Faculty of Science & Technology, University of Twente, IMPACT, PO Box 217, 7500 AE, Enschede, The Netherlands

ARTICLE INFO

Article history:
Received 21 August 2009
Received in revised form 14 October 2009
Accepted 16 October 2009
Available online 27 October 2009

Keywords:
Oxidative catalytic cracking
Hexane
Li/MgO
Promoted Li/MgO
MoO_3–Li/MgO
Bi_2O_3–Li/MgO
V_2O_5–Li/MgO

ABSTRACT

Catalytic oxidative cracking of naphtha is conceptually an alternative process to steam cracking. The performance of sol–gel synthesized Li/MgO in oxidative cracking of hexane as a model compound of naphtha, has been studied and compared to that of conventionally prepared catalyst. At a temperature as low as 575 °C, Li/MgO shows reasonable hexane conversions (28 mol%) and excellent selectivity to light olefins (60 mol%). It is proposed that hexane activation occurs on the catalyst surface *via* the Li^+O^- defect sites, where O^- active sites abstract hydrogen from a secondary carbon atom. The formed hexyl radical in gas phase and in the presence of molecular oxygen will then undergo a complex radical chemistry resulting in a product mixture of C_1–C_5 hydrocarbons (paraffins and olefins) as well as combustion products. Presence of oxygen in the feed is crucial to prevent coking, and to regenerate the catalyst surface through reaction with adsorbed surface hydrogen atoms, thus maintaining catalyst activity. Oxygen also plays a significant role in accelerating radical chemistry in gas phase. Unlike steam cracking, catalytic oxidative cracking results in a relatively higher ratio of high olefins (butylenes + propylene) to ethylene. Thus presence of the catalyst provides a better control over product distribution. Promotion of Li/MgO with MoO_3 and Bi_2O_3 results in considerable improvements in catalyst activity and stability.

1. Introduction

Environmental regulations and attempts towards more energy efficient processes introduce new challenges for the petrochemical industry. Ethylene and propylene are building blocks for the chemical industry. The demand for these olefins is enormous and a growth rate of 4% is predicted for the coming years [1]. Higher growth rate for propylene demand compared to ethylene is expected in the future [1]. Olefin yields from current production technologies are unlike to be able to satisfy these demands.

Steam cracking is the major route for the production of light olefins today. A hydrocarbon feedstock (ethane-to-naphtha) in the presence of steam is cracked to light olefins at high temperatures of 700–900 °C. Steam cracking maximizes the yield of ethylene and $(C_4^= + C_3^=)/C_2^=$ ratios of typically 0.8 are observed [1]. Steam cracking is a highly endothermic reaction, requiring substantial external heat input. Coke deposition on the inner walls of the reactor tubes, inhibiting heat transfer, is also considered a significant issue.

Catalytic oxidative cracking is a potential alternative to steam cracking, because (i) oxidation is exothermic, (ii) the process can be carried out adiabatically and (iii) minimizes coke formation. Liu et al. [2] observed, for the non-catalytic pyrolysis of hexane at 750 °C, that oxygen in the feed (i) accelerated reaction rates resulting in higher conversions of hexane (85 mol%) and (ii) gave reasonable olefin selectivities (59 mol% of light olefins) with ethylene produced as the major product. The presence of oxygen allowed the cracking process to run in an autothermal way, where the exothermic combustion of product hydrogen provided the heat required for cracking internally.

Liu et al. [3] also performed a comparative study of homogeneous gas phase versus heterogeneous catalytic oxidative cracking of hexane at a temperature of 700 °C. Amongst the catalysts tested, 0.25 wt% Li/MgO showed the best performance (64 mol% conversion of hexane, 67 mol% selectivity to olefins). However, the high temperature used in the study, resulted in the domination of gas phase reactions and presence of catalyst had no major influence on conversions of hexane and yields of olefins. In order to use catalysts efficiently, two things are required: (i) need for more active catalysts and (ii) possibility to operate at lower temperatures. Burch and Crabb [4] showed that, for the oxidative conversion of propane, combination of heterogeneous (catalytic) and homogeneous (gas phase) reactions is necessary to obtain commercially acceptable yields of propene. In an earlier study in our laboratory, Leveles et al. [5] justified the use of a catalyst in oxidative dehydrogenation (ODH) of propane in order to have more control over the distribution of products and $C_3^=/C_2^=$ ratios. Moreover, it was shown that in the presence of a catalyst the reaction temperatures can be decreased to 550 °C [5,6].

* Corresponding author. Tel.: +31 53 489 2858; fax: +31 53 489 4683.
E-mail address: l.lefferts@tnw.utwente.nl (L. Lefferts).

0926-860X/$ – see front matter © 2009 Elsevier B.V. All rights reserved.
doi:10.1016/j.apcata.2009.10.030

The development of an efficient oxidation catalyst, however, remains a challenge. The right catalyst should be able to selectively activate the alkane in the presence of the very reactive olefins, thus inhibiting the consecutive deep oxidation of the product olefins. Very little information is reported in literature regarding catalytic oxidative cracking of naphtha range hydrocarbons. Extensive studies have been reported on the development of an efficient catalyst for the oxidative dehydrogenation/cracking of propane/butane. Oxidic catalysts with red–ox properties were mostly attempted and showed limited yields of olefins (<30 mol%) due to the re-adsorption of product olefins and their combustion on the catalyst surface [7–9]. Recent work in our laboratory [5,6] on oxidative conversion of propane clearly highlights non-reducible alkali metal-based oxides such as Li-promoted magnesia (Li/MgO) as promising catalysts. The results show (i) remarkably high olefin yields, as high as 50 mol%, (ii) low combustion yields (<5 mol%), (iii) no aromatic products, and (iv) higher selectivity to propylene than to ethylene. These promising results are due to both basic and non-red–ox properties of the Li/MgO catalyst which prevents further adsorption and hence combustion of the product olefin, respectively. These studies have shown, in agreement with earlier work on methane [10,11] that [Li^+O^-] type defect sites are responsible for catalytic activity. Oxidative cracking of propane follows a radical mechanism where the oxygen defect site on the catalyst surface selectively abstracts hydrogen from the propane. The resulting propyl radicals leave the catalyst surface and follow radical chain reactions in the gas phase. Oxygen has two functions in the mechanism. Firstly, oxygen plays a significant role in the regeneration of the catalyst by removing hydrogen from the surface [Li^+OH^-] species formed during the activation of the alkane. Secondly, oxygen enhances the concentration of chain propagator radicals such as $HO_2^\bullet$ in the gas phase [6].

We showed earlier that nanoclusters of Li/MgO brought considerable improvement in activity for the oxidative conversion of propane [12]. Sol–gel method was applied for the synthesis of these nanoclusters. The advantage of this method over the conventional impregnation preparation route is that it allows the incorporation of Li in the magnesia under milder conditions (during sol–gel transformation) thus avoiding the need to calcine the catalyst at very high temperatures (causing sintering and loss of surface area) for achieving incorporation of Li [12,13]. Li/MgO catalyst prepared with the sol–gel method had (i) higher surface area, (ii) higher concentration of surface [Li^+O^-] sites, and (iii) higher activity than the same catalyst prepared by conventional impregnation method.

In this paper we explore catalytic oxidative cracking of hexane over the newly developed Li/MgO catalyst, and compare performance to that achieved with conventional Li/MgO catalyst. Further, we investigate the possible modification of Li/MgO with small amounts of red–ox promoters to enhance hydrogen abstraction, which is the rate limiting step in oxidative cracking, aiming at improving catalyst activity further and increasing total yields of olefins. V_2O_5, MoO_3 and Bi_2O_3 are selected as promoters. V–MgO and Mo–MgO based catalysts are extensively studied in literature for the oxidative dehydrogenation of C_2–C_4 paraffins [7–9,14–20]. V–MgO catalysts show high dehydrogenation activity at relatively low temperatures (450–550 °C), however selectivities to olefins decrease with conversion due to the secondary combustion of olefins *via* the catalyst surface [9]. Mo–MgO based catalysts however, in comparison to V–MgO catalysts show lower activity but better selectivities to olefins [19,20]. It is reported [18] that oxidative dehydrogenation of C_2–C_4 alkanes over supported transition metal oxides proceeds *via* Mars and van Krevelen mechanism involving lattice oxygen. Bismuth based catalysts are reported in literature [21] as efficient catalysts for the oxidation of propylene to acrolein. Mechanistic studies [21] suggest propylene activation *via* H abstractant by Bi_2O_3 and the consecutive reaction of the formed allyl radical. Moreover, Bi_2O_3 based catalysts have been repeatedly reported by Grasselli et al. [22,23] and Late et al. [24] as selective catalysts for consecutive hydrogen oxidation during the dehydrogenation of light paraffins.

2. Experimental

2.1. Materials

Commercially available $Mg(OCH_3)_2$ solution (Aldrich, 6–8 wt% in methanol), methanol (Merck), $LiNO_3$ (Aldrich, assay ≥99.99%) and MgO (Merck) were used for preparation of Li/MgO catalysts. Ammonium meta-vanadate (Aldrich, 99.999%), ammonium molybdate (Aldrich, 99.98%) and bismuth (III) nitrate pentahydrate (Aldrich, 99.999%) were used as precursors for V_2O_5, MoO_3 and Bi_2O_3 respectively. Pure hexane (Fluka, GC assay ≥99.0%) was used for catalytic experiments.

2.2. Catalyst preparation

The conventional Li/MgO catalyst (Li/MgO IMP) was prepared by wet impregnation of MgO (Merck) with $LiNO_3$ solution, according to the method described in Ref. [5].

Sol–gel synthesized MgO and Li/MgO (Li/MgO SG) catalysts used in this study were prepared according to the method described in Ref. [12]. Modified V_2O_5–Li/MgO, MoO_3–Li/MgO and Bi_2O_3–Li/MgO were prepared by wet impregnation of the sol–gel synthesized Li/MgO using solutions of the metal precursors. The modified catalysts were then dried at 50 °C in vacuum for 7 h and calcined at 600 °C for 5 h. Similarly, both MoO_3–MgO and Bi_2O_3–MgO were prepared by the wet impregnation of the sol–gel synthesized MgO.

2.3. Sample characterization

BET surface area of the catalyst was determined with nitrogen physisorption using a Micro-metrics Tristar Instrument. The samples were out-gassed in vacuum at 250 °C for 24 h prior to the analysis. Elemental composition of Li was determined with atomic absorption spectroscopy (AAS). The composition of Mo, Bi and V oxides was determined with X-ray fluorescence spectroscopy (XRF) (Phillips PW 1480 spectrometer). Results are presented in Table 1.

2.4. Catalytic tests

The catalytic tests were carried out at atmospheric pressure and isothermal conditions in a conventional fixed-bed reactor. An alumina reactor of 4 mm internal diameter was used. The catalyst bed (10 mm length) was packed between two quartz-wool plugs in the alumina reactor. Powder catalyst was pressed, crushed and sieved to the particle size of 0.4–0.6 mm before use. An alumina

Table 1
Surface area (BET) and XRF data of the catalysts.

Catalyst	BET surface area (m^2/g)	Metal oxide loading (wt%)
MgO	176	
MoO_3–MgO	144	0.52
Bi_2O_3–MgO	99	0.68
Li[a]/MgO IMP	8	
Li[a]/MgO SG	76	
MoO_3–Li/MgO	70	0.51
Bi_2O_3–Li[a]/MgO	63	0.63
V_2O_5–Li[a]/MgO	85	1.18

[a] Li content in all samples = 0.86 wt%.

rod of 3 mm internal diameter was placed right below the catalytic bed to reduce the post-catalytic volume in order to minimize homogenous gas phase reactions. A Chromel–Alumel thermocouple inside a quartz tube was inserted above the catalytic bed to record reaction temperature. The temperature of the furnace was controlled by another thermocouple placed outside the reactor tube within the isothermal zone of the tubular furnace.

Reactions were studied in the temperature range between 475 and 600 °C. Total feed of 100 ml/min was used. The feed consisted of 10 mol% of hexane vapor, 8 mol% of O_2 and balance helium (unless stated differently). Before each catalytic test, the catalysts were pretreated in 50% O_2/He (60 ml/min) for 1 h at a temperature of 625 °C. For analysis of the product mixture for every set of experimental conditions, samples were injected to both micro-GCs every 5 min during a period of 5 h. In case of blank experiments, quartz inert (0.4–0.6 mm particle size) was used instead of the catalyst (10 mm bed length).

Mass-flow controllers (Brooks) were used to control the flow of gases. Two electrically actuated 4-port 1-position valves (Valco) were used to switch the reaction mixture to the by-pass line to measure the composition of the feed. Dionex Dual Gradient P680 HPLC pump was used to dose liquid hexane with an accurate rate which was gasified in a cylindrical gasifier operated at a temperature of 130 °C. The temperature of all lines of the setup was kept constant at 130 °C to avoid condensation of hexane.

The online analysis system consisted of two micro-GCs (Varian CP4900). The first micro-GC is a quad system consisting of four channels with four different columns. Column 1: Molsieve 5A Plot (He carrier gas) for the separation of O_2, N_2, CH_4 and CO, Column 2: PoraPlot Q for the separation of CO_2, C_2H_6, C_2H_4, H_2O, Column 3: alumina KCl plot at $T = 80$ °C for the separation of C_3 and C_4 hydrocarbons (paraffins and olefins), Column 4: alumina KCl plot at $T = 160$ °C for the separation of C_5 hydrocarbons (paraffins and olefins). The second micro-GC is a dual system consisting of two channels of two different columns. Column 1: Molsieve 5A Plot (Ar carrier gas) for the separation of He and H_2, Column 2: CP-SIL 5CB for the separation of C_6–C_8 hydrocarbons both paraffins and olefins. All channels used TCD detectors. This elaborate GC system allows full analysis of C_1–C_8 hydrocarbons both paraffins and olefins.

A gas mixture of known concentrations of C_1–C_6 hydrocarbons (paraffins and olefins) was used for the calibration of the micro-GCs. Table 2 presents a typical analysis of product mixture. Hexane conversions were calculated on a carbon mol basis; i.e. (in case of the hexane) (C_{6in} moles − C_{6out} moles)/C_{6in} moles × 100%. The carbon balance closed between 100% and 105%. Selectivity to individual products was also calculated based on the number of moles of carbon contained in the products, divided by the total number of moles of carbon in the product mixture excluding unconverted feed; i.e. $(n_iC_i/\sum n_iC_i) \times 100\%$. Selectivity to both H_2 and H_2O was similarly calculated based on the number of moles of H contained in each divided by the total number of moles of hydrogen in the product mixture excluding unconverted feed; i.e. $(n_iH_i/\sum n_iH_i) \times 100\%$.

Table 2
Typical analysis of product mixture of a catalytic experiment.

Component	Concentration (mol%)	Component	Concentration (mol%)
Oxygen	2.828	iso-Pentane	0.023
CO	1.47	n-Pentane	0.0025
CO_2	2.303	3-Methyl-1-Butene	0.01
Methane	0.288	trans-2-Pentene	0.01
Ethane	0.095	2-Methyl-2-Butene	0.205
Ethylene	1.785	2-Methyl-1-Butene	0.125
Propane	0.048	cis-2-Pentene	0.01
Propylene	1.33	Hexane (unconverted)	7.075
iso-Butane	0.038	Hydrogen	2.39
n-Butane	0.05	Water	6.575
1-Butene	0.425	He balance	72.9
cis-2-Butene	0.015		

2.5. Temperature programmed desorption

In situ CO_2 TPD was performed after catalyst testing (or after catalyst pretreatment) from 100 to 950 °C with an increment of 10 °C/min, with He flow of 10 ml/min as a carrier gas. The catalyst sample (100 mg) was allowed to stay isothermally at 950 °C for half an hour. The concentration of desorbed CO_2 was determined with the quad micro-GC (PPQ column) every 2 min.

3. Results

3.1. Influence of temperature on the performance of Li/MgO

Table 3 shows results of the catalytic oxidative cracking of hexane in the temperature range 475–575 °C, both with the conventionally and the sol–gel synthesized Li/MgO. Both catalysts showed activity at temperatures as low as 475 °C, however, experiments with inert quartz (not shown here) showed measurable hexane conversions only at temperatures above 600 °C. Compared to the conventional catalyst, the sol–gel synthesized Li/MgO showed improved performance, i.e. higher hexane conversions and better selectivities to C_2–C_4 olefins, at almost all temperatures. The sol–gel Li/MgO is further investigated in this paper for the oxidative cracking of hexane.

Results in Table 3 show clearly the influence of temperature on product distribution. With the increase in temperature we observe dramatic decrease in the formation of both H_2O and CO_x and increase in the formation of (oxi-) cracking products (C_2H_4, C_3H_6 and C_4 olefins) as well as C_1–C_5 paraffins. Hydrogen varied only slightly with temperature and a maximum was observed at 525 °C. In addition, temperature influences the relative concentrations of olefins formed during the oxidative conversion of hexane. Ratio of $(C_4^= + C_3^=)/C_2^=$ decreased with increasing temperature due to the consecutive cracking of C_3–C_4 olefins to ethylene. At 575 °C formation of more $C_4^= + C_3^=$ than $C_2^=$ can still be achieved ($(C_4^= + C_3^=)/C_2^=$ mol/mol = 1.6). This ratio would be typically about 0.8 under steam cracking conditions [1,25]. Since best selectivities

Table 3
Performance of Li/MgO catalysts during oxidative conversion of hexane (reaction conditions: 100 ml/min, 10% hexane, 8% oxygen and balance He; WHSV = 15.4 h^{-1}).

	475		525		575	
	Li/MgO		Li/MgO		Li/MgO	
	(IMP)	(SG)	(IMP)	(SG)	(IMP)	(SG)
Conversion (mol%)						
Hexane	3.82	4.19	9.92	11.17	24.49	28.35
Oxygen	24.40	23.57	49.44	42.67	92.18	65.19
Selectivity based on C (mol%)						
CO	40.33	41.16	32.30	24.86	12.79	9.57
CO_2	49.70	41.31	35.74	27.21	24.20	14.99
CH_4	0.00	0.00	0.53	0.57	1.53	1.87
C_2H_4	1.89	2.20	5.34	9.54	18.36	23.24
C_3H_6	4.27	6.76	10.81	18.88	20.04	25.97
$C_{4s}^=$ (butylenes)	3.79	5.81	10.35	12.21	12.23	11.46
C_2–C_4 paraffins	0.00	0.00	0.45	0.38	3.68	4.44
C_{5s} (paraffins and olefins)	0.00	2.75	4.48	6.36	7.17	8.46
$(C_4^= + C_3^=)/C_2^=$	4.26	5.70	3.97	3.26	1.76	1.61
Selectivity based on H (mol%)						
H_2	9.28	11.80	10.47	13.79	7.84	11.30
H_2O	85.60	78.78	70.27	55.26	49.53	31.19

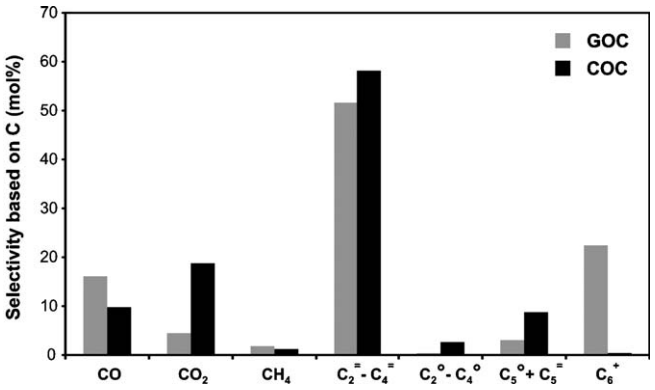

Fig. 1. Gas phase oxidative cracking (GOC) *vs.* catalytic oxidative cracking (COC) over Li/MgO SG. Conversion: 30 mol% hexane. Reaction conditions: 100 ml/min, 10% hexane, 20% oxygen and balance He, T = 575 °C.

were achieved at 575 °C and since above this temperature gas phase activation of hexane starts to be significant, we chose this as the optimal temperature for studying the influence of the catalyst. This is much lower than the temperature commonly used for naphtha steam cracking to generate olefins (>700 °C).

3.2. Role of catalyst in controlling product distribution

Catalytic oxidative cracking (COC) over Li/MgO SG catalyst shows a product distribution that is different from that of gas phase oxidative cracking (GOC) at the same temperature. As shown in Fig. 1, GOC resulted in the formation of higher amounts of products $\geq C_6$ (most probably aromatics, they could not be separated by the GC columns used) than COC. With catalytic cracking we observe formation of more light olefins ($C_2^=-C_4^=$) as well as more C_5 hydrocarbons (mainly olefins). The catalyst provides for more olefin, than in the absence of catalyst. CO_x production from COC is still significantly higher as compared to GOC because of CO_2 production due to deep oxidation *via* the catalyst surface. Hence further improvement of catalyst selectivity is necessary. Further, at 575 °C, olefin selectivity was invariant with the hexane conversion level. Fig. 2 shows that increase in hexane conversions from 15% to 45%, caused only marginal changes. High selectivities to olefins were maintained, with even slight decrease in selectivities to CO_x. Different levels of hexane conversion were achieved by varying weight-hourly-space velocity (WHSV).

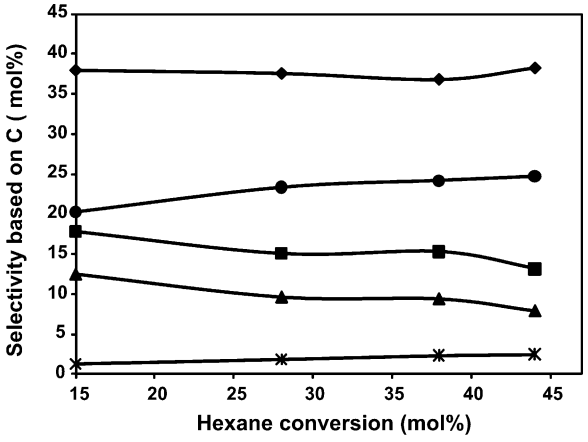

Fig. 2. Selectivity to different products *vs.* hexane conversion with Li/MgO SG. (◆) ($C_3^= + C_4^=$), (●) C_2H_4, (■) CO_2, (▲) CO, and (*) CH_4. Reaction conditions: 100 ml/min, 10% hexane, 8% oxygen and balance He. Different conversions achieved by varying WHSV from 5 to 102 h^{-1}.

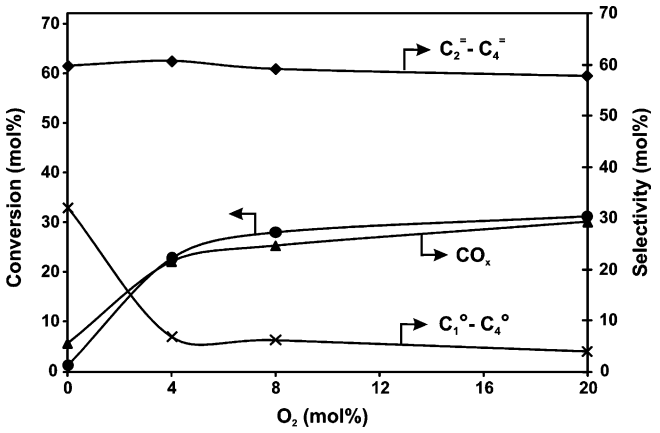

Fig. 3. Influence of oxygen concentrations on hexane conversions as well selectivity to products. (●) Hexane conversion, (▲) selectivity to CO_x, (◆) selectivity to light olefins ($C_2^=-C_4^=$), (×) selectivity to C_1–C_4 paraffins (C_1°–C_4°). Oxygen conversions = 68.5, 65.2 and 38.5 mol% at 4, 8 and 20 mol% O_2, respectively. Reaction conditions: 100 ml/min, 10% hexane and balance He, T = 575 °C. WHSV = 15.4 h^{-1}. Catalyst studied is Li/MgO SG.

3.3. Influence of oxygen concentrations in the feed

The influence of oxygen concentrations in the feed on both hexane conversions and selectivities to products has been as well investigated. Fig. 3 shows that the increase in oxygen concentrations induced a significant increase in the conversion of hexane. In the absence of oxygen, hexane conversions were negligible. Increasing oxygen concentrations in the feed introduced only a slight decrease in selectivity to light olefins $C_2^=$, $C_3^=$, and $C_{4s}^=$, i.e. from 62 to 60 mol%. In the low oxygen range (0–4%), increase in selectivity to CO_x was observed, at the expense of C_1–C_4 paraffins. For oxygen concentrations above 4 mol%, changes to CO, CO_2 and C_1–C_4 paraffin selectivities were only marginal.

Selectivities to products with varying oxygen concentrations were further investigated, keeping the hexane conversion constant by varying WHSV (Fig. 4). At the higher oxygen concentrations (20 mol%) an increase in CO_x selectivity (22–38 mol%) accompanied by a slight decrease in selectivities to both olefins (63–

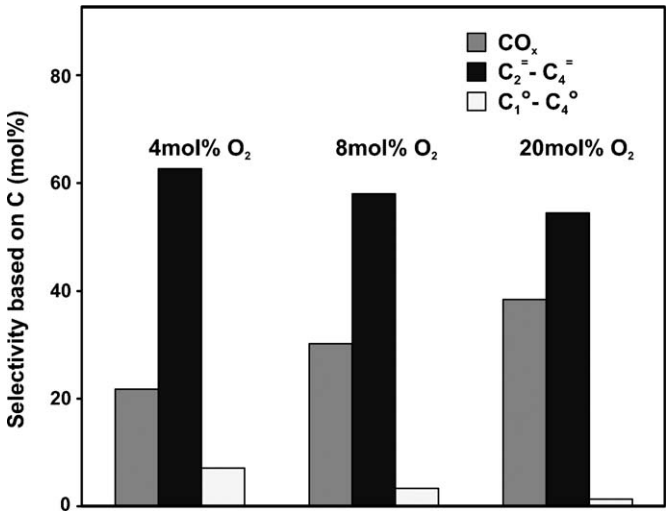

Fig. 4. Influence of oxygen concentrations on selectivity to CO_x, C_2–C_4 olefins ($C_2^=-C_4^=$) and C_1–C_4 paraffins (C_1°–C_4°) at hexane conversion of 17 mol%. Oxygen conversions = 68.5, 40.5 and 23.5 mol% at 4, 8 and 20 mol% O_2, respectively. Reaction conditions: 100 ml/min, 10% hexane and balance He, T = 575 °C. WHSV = 15.4–44 h^{-1}. Catalyst studied is Li/MgO SG.

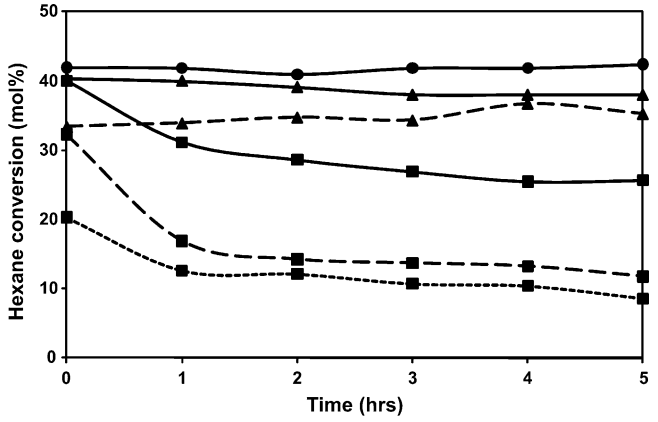

Fig. 5. Hexane conversion as function of time-on-stream. (■) Li/MgO SG, (▲) MoO_3–Li/MgO, (●) Bi_2O_3–Li/MgO. (Solid lines) without CO_2 in the feed, (dashed lines) co-feeding 5 mol% of CO_2, (dotted line) co-feeding 10 mol% of CO_2. Reaction conditions: 100 ml/min, 10% hexane, 8% oxygen and balance He, T = 575 °C. WHSV = 15.4 h^{-1}.

54 mol%) and C_1–C_4 paraffins was observed. Generally, with increasing oxygen amounts in the feed there is a continuous increase in amount of CO_x produced, specifically an increase in CO_2 production ($CO_2/CO > 1$).

3.4. Stability of Li/MgO SG catalyst

The activity of Li/MgO SG catalyst during a typical experiment is shown in Fig. 5. Partial deactivation was observed within the first 1 h of time on stream. After this the catalytic activity was almost stable. Temperature programmed desorption of CO_2 was performed on the used Li/MgO SG (after test for 5 h) and compared to that of a fresh catalyst pretreated in oxygen at 625 °C (Fig. 6). TPD of the fresh catalyst showed a typical CO_2 desorption peak of Li_2CO_3 at 860 °C [26,27]. The presence of Li_2CO_3 (formed with CO_2 from ambient) is an inherent property of Li/MgO [28]. TPD of the used catalyst however, showed a broad CO_2 desorption peak with a maximum at 690 °C followed by a second peak around 900 °C. The broad CO_2 desorption peak at 690 °C is most likely attributed to CO_2 adsorbed on Li^+O^- active sites ($Li^+CO_3^-$) [27,29], and suggests that part of the adsorbed CO_2 is responsible for the observed poisoning effect. The higher concentration of Li_2CO_3 observed in the used catalyst would possibly indicate that the surface carbonate phase, $Li^+CO_3^-$, further reacts with Li^+O^- active sites, thus accelerating the segregation of Li from these active sites in the form of Li_2CO_3. Indeed, co-feeding 5 mol% of CO_2 in an experiment with fresh catalyst resulted in a steeper decrease in hexane conversions as shown in Fig. 5. The negative influence of CO_2 on catalyst activity has been further confirmed by co-feeding up to 10 mol% of CO_2. CO_2 has a poisoning effect on the catalyst as indicated in Fig. 5, addition of up to 10 mol% of CO_2 to the feed, introduced a decrease in initial hexane conversion from 40 to 20 mol%.

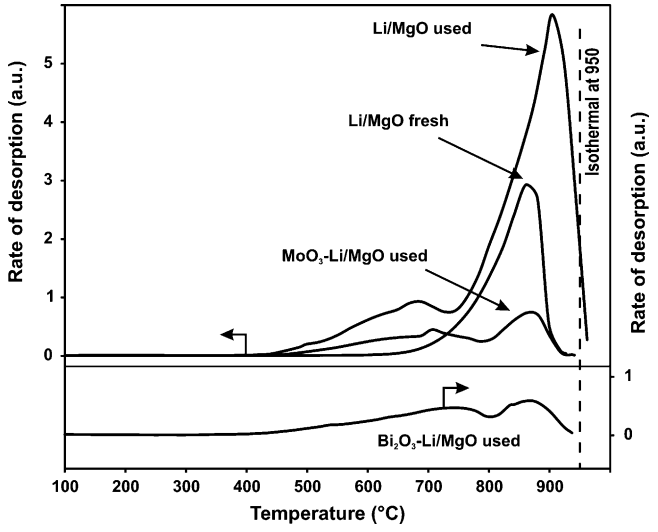

Fig. 6. Temperature programmed desorption of CO_2 for fresh and used catalysts (TPD in situ after catalytic reaction, signals are normalized to the BET surface area). Temperature ramp 10 °C/min, He 10 ml/min.

Table 4
Influence of post-catalytic volume (reaction conditions: 100 ml/min, 10% hexane, 8% oxygen and balance He; WHSV = 15.4 h^{-1}).

	Without post-catalytic volume	With post-catalytic volume
Conversion, mol%		
Hexane	28.35	33.59
Oxygen	65.19	65.49
Product selectivity, mol%		
CO_x	24.56	20.48
CH_4	1.87	2.27
C_2–C_4 olefins	60.67	63.31
C_2–C_4 paraffins	4.44	5.04
C_{5s} (paraffins and olefins)	8.46	8.90

3.5. Influence of post-catalytic volume

Combining catalytic reaction with a post-catalytic thermal reaction (post-catalytic void of 3.6 cm^3) introduced an increase in hexane conversions from 28 to 33 mol% as well as slight improvement in selectivity to light olefins from 60 to 63 mol%. Results are shown in Table 4.

3.6. Modification of Li/MgO catalyst

In order to improve catalyst activity further, hence yields of olefins, we modified Li/MgO SG with small amounts of red–ox promoters. Fig. 7 shows yields of C_2–C_4 olefins at 575 °C with MoO_3, Bi_2O_3 and V_2O_5 promoted MgO and Li/MgO catalysts, initially and after time on stream.

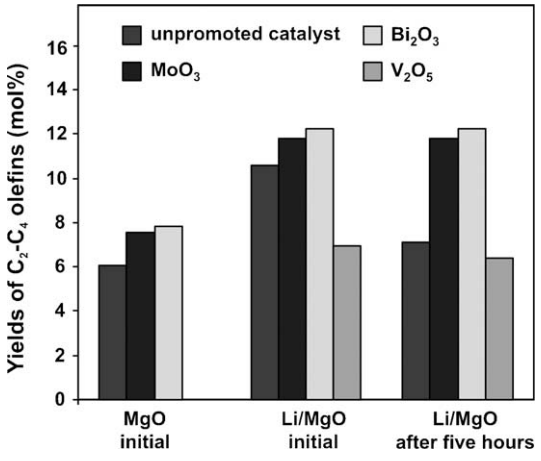

Fig. 7. Yields of C_2–C_4 olefins for MgO, Li/MgO SG and MoO_3, Bi_2O_3, V_2O_5 promoted catalysts, initially (at minute 5) and after 5 h of time on stream. Initial hexane conversions (minute 5): 12.07%, 12.58%, 14.80%, for MgO, MoO_3–MgO, Bi_2O_3–MgO, respectively. 19.12%, 23.00%, 20.93%, 18.13% for Li/MgO SG, MoO_3–Li/MgO, Bi_2O_3–Li/MgO and V_2O_5–Li/MgO, respectively. Reaction conditions: 100 ml/min total flow, 10% hexane, 8% oxygen and He balance, T = 575 °C. WHSV = 154 h^{-1}.

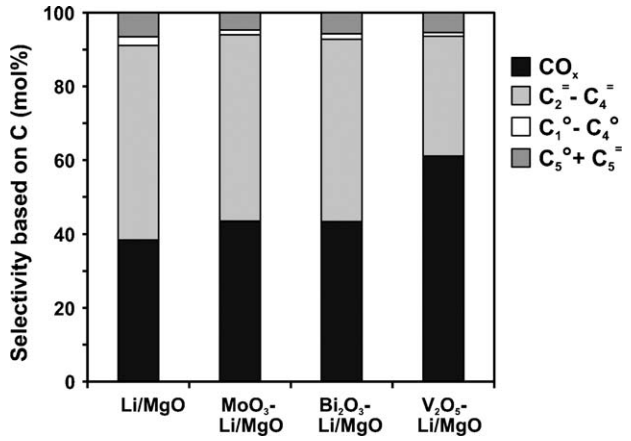

Fig. 8. Selectivity to products based on C at hexane conversion of 10 mol%. Oxygen conversions = 35 mol% (Li/MgO SG), 37 mol% (MoO_3–Li/MgO), 44 mol% (Bi_2O_3–Li/MgO), and 70 mol% (V_2O_5–Li/MgO). Reaction conditions: 100 ml/min total flow, 10% hexane, 8% oxygen and He balance, T = 575 °C. WHSV = 154–385 h^{-1}.

As compared to Li/MgO both MoO_3–Li/MgO and Bi_2O_3–Li/MgO resulted in higher yields of light olefins. This improvement in the yields of olefins was more significant after 5 h of reaction because Li/MgO catalyst lost activity with time (as shown in Fig. 5). Moreover interestingly, addition of 0.52 wt% MoO_3 and 0.68 wt% Bi_2O_3 to MgO as well resulted in better yields than MgO. Generally, in the MoO_3 and Bi_2O_5 promoted catalysts the observed higher yields of olefins, were the results of enhancement in hexane conversions without any significant changes in selectivity to products. V_2O_5–Li/MgO, however showed the minimum yields of olefins. Fig. 8 shows the selectivities based on carbon to different products at 575 °C with the four catalysts; Li/MgO, MoO_3–Li/MgO, Bi_2O_3–Li/MgO and V_2O_5–Li/MgO at similar hexane conversion of 10 mol%. Similar hexane conversions were achieved by varying WHSV. V_2O_5–Li/MgO resulted in the formation of more combustion products, while both MoO_3–Li/MgO and Bi_2O_3–Li/MgO showed similar selectivities as Li/MgO. Selectivities to products based on hydrogen (Fig. 9) however, showed slight differences between Bi_2O_3–Li/MgO and MoO_3–Li/MgO. Bi_2O_3–Li/MgO resulted in formation of more water and less hydrogen than both Li/MgO and MoO_3–Li/MgO.

The stability of MoO_3 and Bi_2O_3 promoted Li/MgO has been as well investigated both with and without the presence of CO_2 in the feed. The promoted catalysts maintained complete activity. The presence of 5 mol% of CO_2 with MoO_3–Li/MgO did not influence catalyst activity unlike Li/MgO (Fig. 5). Fig. 6 shows the temperature programmed desorption of CO_2 for MoO_3–Li/MgO and Bi_2O_3–Li/MgO catalysts after testing in comparison to that of used Li/MgO. CO_2 desorption from the promoted catalysts showed the same trend as the unpromoted catalyst however with much smaller desorption peaks.

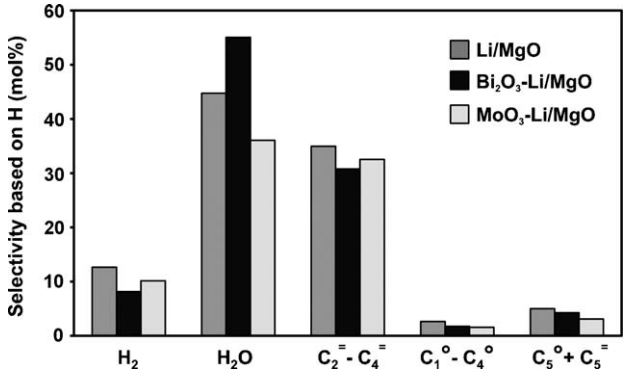

Fig. 9. Selectivity to products based on H at hexane conversion of 10 mol%. Oxygen conversions = 35 mol% (Li/MgO SG), 37 mol% (MoO_3–Li/MgO) and 44 mol% (Bi_2O_3–Li/MgO). Reaction conditions: 100 ml/min total flow, 10% hexane, 8% oxygen and He balance, T = 575 °C. WHSV = 154–385 h^{-1}.

4. Discussion

Li/MgO catalyst is active for oxidative cracking of hexane at temperatures as low as 475 °C. In the absence of the catalyst measurable hexane conversions were noticed only at $T \geq 600$ °C. In the absence of catalyst, homogeneous activation occurs *via* hydrogen abstraction by gas phase diatomic oxygen, forming $HO_2^{\bullet}$ radicals (reaction (1)) [2,30,31].

$$C_6H_{14} + O_2 \rightarrow C_6H_{13}^{\bullet} + HO_2^{\bullet} \quad \text{(gas phase, homogeneous)} \quad (1)$$

At 575 °C hexane conversion was 25 mol% with the conventional catalyst and 28 mol% with the sol–gel synthesized Li/MgO (Table 3). Influence of the presence of catalyst Li/MgO on the activation of hexane is significant. As mentioned in Section 1, $[Li^+O^-]$ type defect sites are responsible for catalytic activity of Li/MgO catalyst [10–13]. In the case of oxidative conversion of propane, we have shown earlier [6] that hydrocarbon activation occurs *via* a radical mechanism involving homolytic scission of C–H bonds. The oxygen of the $[Li^+O^-]$ defect site on the catalyst surface selectively abstracts a hydrogen from propane, forming $[Li^+OH^-]$ on the surface and releasing a propyl radical to the gas phase (reaction (2)). As in the case of propane we propose that the first step in the activation of hexane is the abstraction of a hydrogen and formation of hexyl radicals (reaction (2)). Further reactions of hexyl radicals take place in the gas phase.

$$C_6H_{14} + O^-{}_s \rightarrow C_6H_{13}^{\bullet} + OH^-{}_s \quad \text{(catalytic, heterogeneous)} \quad (2)$$

The sol–gel synthesized Li/MgO showed improved performance at almost all temperatures. The relatively better performance of this catalyst as compared to the conventional catalyst is in agreement with results we have reported earlier during the ODH of propane [12,13]. This improvement is attributed to the higher concentration of Li^+O^- sites in the sol–gel synthesized Li/MgO.

Generally, with the sol–gel synthesized Li/MgO, cracking reactions and olefin formation were more significant at $T > 525$ °C while at lower temperatures CO_x formation was more dominant. This improvement in selectivity to olefins with temperature is explained with the fact that the rates of radical chain propagation reactions increase with temperature, thus increasing the ratio of homogenous to heterogeneous reactions of these radicals [6]. At low temperatures radicals initiated on the catalyst surface most likely interact with unselective O^{2-} sites of MgO forming alkoxy species as precursors for CO_x. Reaction of hydrocarbon radicals with surface oxygen has been reported to lead to surface alkoxy species ($C_nH_{2n+1}O^-{}_s$) (reaction (3)), and an electron trapped at an oxide ion vacancy (VO″) [10,33]. Such species are reported for a variety of paraffins/olefins (ethane [8], C_1–C_4 paraffins [33], C_2–C_4 olefins [34]) during oxidation reactions. Alkoxide species are reactive and known to be intermediates in total oxidation pathways through consecutive attack by gas phase oxygen (reaction (4)) [10,31,33]. In comparison to C_1–C_4 paraffins/olefins, the radical chemistry during oxi-cracking of hexane is expected to be even more complex because a variety of radicals are formed. However, we assume that deep oxidation reactions follow the same pathways as suggested earlier for lower paraffins [7,10,11,31].

$$C_nH_{2n+1}^{\bullet} + O^{2-}{}_s \rightarrow C_nH_{2n+1}O^-{}_s + e^- \quad (n \leq 6) \quad (3)$$

$$C_nH_{2n+1}O^-{}_s + O_2 + e^- \rightarrow CO, CO_2, H_2O + O^{2-}{}_s \quad (4)$$

At temperatures above 525 °C, desorption of radicals formed by hydrogen abstraction, is thermodynamically more favored than reaction with surface oxygen for alkoxide formation. This might be the reason that at higher temperatures, lower selectivities to CO_x (Table 3) are observed. Similarly with the increase in temperature, water concentrations decreased as result of decrease in extent of combustion reactions. Hydrogen formation showed a maximum at 525 °C, most probably due to the lower severity of cracking at this relatively low temperature while at the higher temperature (575 °C) cracking reactions and olefin formation were more dominant. Generally, during both oxidative dehydrogenation and cracking reactions occurring in gas phase in the presence of molecular oxygen, possible pathways for H_2 formation are the termination reactions of $H^{\bullet}$ radicals and/or addition reactions of alkyl and $H^{\bullet}$ radicals [35].

Similar to results of our previous work on the oxidative conversion of propane [5,6,12,13], during the oxidative conversion of hexane with Li/MgO olefin selectivity was almost invariant with the hexane conversion level (Fig. 2). Moreover interestingly, selectivity to CO_x slightly decreased with hexane conversions, most probably due to the increase in ratio of homogenous gas phase to heterogeneous surface reactions. The concentration of surface initiated hexyl radicals will determine the extent of gas phase radical chemistry. Thus accelerated gas phase radical chemistry is expected at the higher hexane conversions, where oxygen is selectively involved in reactions with intermediate radicals resulting in the formation of more of olefins and less CO_x. Typically for red–ox-type catalysts, increasing conversion leads to higher combustion and lower olefin selectivities [7,8]. Our results demonstrate that oxidative cracking of hexane over Li/MgO does not suffer from consecutive deep oxidation reactions, similar to ethane, propane and butane [5,6,12,13].

Besides radical initiation, Li/MgO catalyst also contributes in controlling selectivity to olefins; i.e. ratio of higher olefins to ethylene $(C_4^= + C_3^=)/C_2^=$. At 575 °C ratio of $(C_4^= + C_3^=)/C_2^=$ (mol/mol) is 1.6. This would be typically about 0.8 under steam cracking conditions [1,25] mainly due to the severity of cracking at the elevated temperatures (>700 °C). Moreover, thermal cracking of naphtha during steam cracking is unselective and variant types of radicals (primary, secondary) are initiated. However, at the presence of strong hydrogen abstractant, in this case O^- site, there is preference for hydrogen abstraction from a secondary carbon atom forming secondary radicals. This preference is due to the relative stability of radical on a secondary carbon atom versus on a primary carbon atom. Previously, Kondratenko and Sinev [36] has shown the role of surface O^- sites (for example $[Li^+O^-]$ in Li/MgO) as strong H abstractants and their preference towards hydrogen abstraction from the secondary carbon atom of propane, thus leading to more dominant formation of iso-propyl radicals. Similarly, in the case of hexane the higher selectivity to C_3, C_4 olefins indicate involvement of the catalyst in the process and the related preference for hydrogen abstraction from a secondary carbon atom forming iso-hexyl radicals. β-Scission of iso-hexyl radicals at this relatively mild cracking conditions (T = 575 °C) will result in higher ratio of high olefins to ethylene. In addition, presence of the catalyst inhibits the formation of $\geq C_6$ products unlike the case of gas phase oxidative cracking.

Oxygen in the feed has significant influence on hexane conversions. In the absence of oxygen, hexane conversions were negligible; this may be due to the fact that regeneration of active sites after one turn over (resulting in the formation of Li^+OH^-) is not possible. Consequently, a steep increase in conversion was observed when adding a low amount of oxygen, *via* regeneration of the sites responsible for radical formation (Fig. 3). Additionally, with the presence of oxygen formation of a new type of chain propagator $[HO_2^{\bullet}]$ radical is favored, enhancing activation of hexane in the gas phase with further increase in oxygen concentrations. Similar observations were made by us earlier [6] during the ODH of propane. Presence of oxygen in the feed is, thus crucial for the following reasons; (i) to prevent coke formation (catalyst in the absence of oxygen was completely covered with coke, hence presence of oxygen is crucial to prevent catalyst deactivation), (ii) to increase conversions hence increase olefin yields, through regeneration of active sites and (iii) to accelerate radical chain chemistry in the gas phase.

Nevertheless, optimum oxygen concentrations are necessary. Increasing the oxygen concentrations slightly shifts product distribution towards the formation of more CO_x. We speculate that this is mainly due to an increase in the formation of intermediate oxygenates which further oxidize, either in gas phase or *via* the catalyst surface. As gas phase oxidative cracking, at similar conditions, gave more CO than CO_2 (Fig. 1), our results indicate that even at these temperatures surface oxidation pathways still contribute significantly.

A drawback of Li/MgO catalyst however, is that it suffers from partial deactivation within the first 1 h of time on stream. It is believed that CO_2 produced during reaction poisons the Li^+O^- active sites of the catalyst. It is reported in literature [6,26,27,29] that CO_2 produced during reaction, interacts with the active sites $[Li^+O^-]$ of the catalyst forming surface intermediate carbonate phase $[Li^+CO_3^-]$, which reacts further with Li^+O^- to form bulk Li_2CO_3 (reaction (5)), deactivating the catalytic sites:

$$Li^+O^- + CO_2 \leftrightarrow Li^+CO_3^- + Li^+O^- \rightarrow Li_2CO_3 + 1/2O_2 \quad (5)$$

In situ CO_2 TPD results (Fig. 6) of the used catalyst compared to the fresh pretreated catalyst, confirmed the presence of both $Li^+CO_3^-$ and Li_2CO_3 phases. Thus, under our reaction conditions carbonates certainly exist, affecting catalyst activity.

The contribution of non-catalytic homogenous gas phase reactions in ODH of paraffins has been repeatedly discussed in literature [7,30–32]. In our experiments combining catalytic reaction with post-catalytic homogenous reactions induced an increase in hexane conversion and olefin yield (Table 4). In both experiments (with and without post-catalytic volume) similar oxygen conversions were observed. The formation of less CO_x in the experiment with post-catalytic volume suggests that oxygen was selectively involved in accelerating the radical chemistry in gas phase in the post-catalytic region, thus resulting in higher hexane conversions. The same trend was observed previously both by us [6] and Nguyen and Kung [32] in ODH of propane, Lemonidou and Stambouli [30] in ODH of n-butane as well as Sinev for ODH of C_3–C_4 paraffins [31]. The higher yields confirm that intermediate radicals desorb from the catalyst surface, initiating radical chain gas phase reaction in the post-catalytic volume. Under our conditions, the effect is positive, improving yields by about 20%.

Modification of Li/MgO with both MoO_3 and Bi_2O_3 resulted in higher yields of C_2–C_4 olefins than promotion with V_2O_5. V_2O_5 showed activity towards unselective combustion reactions of, most probably, intermediate radicals or product olefins. This performance of V_2O_5 is not surprising as it possesses strong red–ox properties resulting in high oxygen conversions and high selectivities to combustion products. V_2O_5 based catalysts have been repeatedly reported in literature as active yet unselective catalysts for ODH of lower hydrocarbons [7–9].

Mo–MgO catalysts however, were reported to be more selective than V–MgO catalysts. Mo doped V–MgO during the oxidative dehydrogenation of propane [20] and n-butane [19] showed better selectivities to olefins. It is believed that C–H bond scission from the alkane during oxidative dehydrogenation of C_2–C_4 alkanes over Mo oxides proceeds *via* Mars and van Krevelen mechanism involving lattice oxygen [18]. Bi_2O_3 is also reported in literature [21] as selective H abstractant during oxidation of propylene to

acrolein. The slight improvement in initial activity, thus initial yields of olefins (Fig. 7), observed during the oxidative conversion of hexane in our experiments both with MoO_3 and Bi_2O_3 promoted catalysts as compared to the unpromoted ones (MgO, Li/MgO), might be attributed to activity of MoO_3 and Bi_2O_3 for C–H bond scission in hexane. The significantly higher yield of olefins at longer time on stream in the case of MoO_3–Li/MgO and Bi_2O_3–Li/MgO, is a result of the better stability of these catalysts as compared to Li/MgO. Based on the observations of CO_2 TPD experiments (Fig. 6), we suggest that both MoO_3 and Bi_2O_3, being Lewis acidic, minimize CO_2 sorption (less formation of Li_2CO_3) and thus prevent poisoning of the Li^+O^- active sites of the catalyst. MoO_3 promoted Li/MgO is selected for further characterization work and is currently under investigation. We will study the influence of varying loadings of MoO_3 on the performance of Li/MgO during the oxidative cracking of hexane, as well as the effect of MoO_3 on the Li^+O^- active sites.

The higher amounts of water formed with Bi_2O_3–Li/MgO in our experiments indicate enhanced hydrogen oxidation. This agrees well with results reported by both Grasselli et al. [22,23] and Late et al. [24] on the ability of Bi_2O_3 for selective hydrogen oxidation.

Generally, results obtained in this study show that catalytic oxidative cracking achieves the following advantages over the conventional steam cracking: (i) lowering reaction temperatures, (ii) increasing the ratio of (butylenes and propylene) to ethylene from 0.8 for steam cracking to 1.6 for oxidative cracking, and (iii) catalytic oxidative cracking is free of any coke formation. However, the formation of combustion products suggests further improvement in catalyst performance.

5. Conclusions

Li/MgO catalyst is active for oxidative cracking of hexane, shows minimal combustion, and gives excellent selectivity to olefins (60 mol%). Sol–gel synthesized Li/MgO shows better performance than the conventionally prepared catalyst due to the higher concentration of Li^+O^- active sites in the latter. It is proposed that catalytic oxidative cracking of hexane is heterogeneously initiated at the $[Li^+O^-]$ active site of the catalyst. This occurs *via* homolytic C–H bond splitting and formation of radicals which undergo reactions in the homogeneous phase. Increasing hexane conversion does not have any detrimental effect on olefin selectivities, thus high olefin yields can be achieved. This behavior is similar to oxidative cracking of lower paraffins over Li/MgO.

Oxygen plays a significant role in regenerating the active sites and accelerating the radical chemistry. It also inhibits coke formation. Higher oxygen concentrations have a minor influence on olefin selectivity.

Active sites of the catalyst are susceptible for deactivation due to poisoning by product CO_2, which interacts with the Li^+O^- sites forming stable Li_2CO_3. Both MoO_3 and Bi_2O_3 promoted Li/MgO, however, maintain activity and show considerably higher yields of C_2–C_4 olefins than Li/MgO during time on stream due to less formation of Li_2CO_3. Bi_2O_3 is selective in the consecutive oxidation of product hydrogen in the presence of olefins.

We conclude that in the oxidative cracking of hexane, Li/MgO shows a similar behavior as in oxidative dehydrogenation of propane; i.e. heterogeneously initiated homogeneous reaction. Selectivities obtained (60 mol% of light olefins and 25 mol% of CO_x) are similar with those achieved during oxidative cracking of C_2–C_4 paraffins [6]. However, hexane is clearly more active than C_2–C_4 paraffins, consequently it is possible to operate at lower reaction temperatures, much lower than temperatures used in conventional steam cracking.

Acknowledgments

The authors gratefully thank ASPECT program, the Netherlands, for financial support (project number 053.62.011). The authors also acknowledge Ing. B. Geerdink and K. Altena-Schildkamp for technical support, L. Vrielink for BET and XRF measurements, Arnau Carné Sánchez for contributing in experimental work and Dr. G. Meima (Dow Benelux) for AAS measurements.

References

[1] T. Ren, M. Patel, K. Blok, Energy 31 (2006) 425–451.
[2] X. Liu, W. Li, H. Xu, Y. Chen, React. Kinet. Catal. Lett. 81 (2) (2004) 203–209.
[3] X. Liu, W. Li, H. Zhu, Q. Ge, Y. Chen, H. Xu, Catal. Lett. 94 (1–2) (2004) 31–36.
[4] R. Burch, E. Crabb, Appl. Catal. A 100 (1993) 111–130.
[5] L. Leveles, K. Seshan, J.A. Lercher, L. Lefferts, J. Catal. 218 (2003) 307–314.
[6] L. Leveles, K. Seshan, J.A. Lercher, L. Lefferts, J. Catal. 218 (2003) 296–306.
[7] F. Cavani, N. Ballarini, A. Cericola, Catal. Today 127 (2007) 113–131.
[8] F. Cavani, F. Trifiro, Catal. Today 24 (1995) 307–313.
[9] M.V. Landau, M.L. Kaliya, A. Gutman, L.O. Kogan, M. Herskowitz, P.F. van den Oosterkamp, Stud. Surf. Sci. Catal. 110 (1997) 315–326.
[10] T. Ito, J.-X. Wang, C.-H. Lin, J.H. Lunsford, J. Am. Chem. Soc. 107 (1985) 5062–5068.
[11] C.-H. Lin, K.D. Campbell, J.-X. Wang, J.H. Lunsford, J. Phys. Chem. 90 (4) (1986) 534–537.
[12] C. Trionfetti, I.V. Babich, K. Seshan, L. Lefferts, Appl. Catal. A 310 (2006) 105–113.
[13] C. Trionfetti, I.V. Babich, K. Seshan, L. Lefferts, Langmuir 24 (2008) 8220–8228.
[14] M.A. Chaar, D. Patel, M.C. Kung, H.H. Kung, J. Catal. 105 (1987) 483–498.
[15] M.A. Chaar, D. Patel, H.H. Kung, J. Catal. 109 (1988) 463–467.
[16] K.T. Nguyen, H.H. Kung, Ind. Eng. Chem. Res. 30 (1991) 352–361.
[17] D. Siew Hew Sam, V. Soenen, J.C. Volta, J. Catal. 123 (1990) 417–435.
[18] E. Heracleous, M. Machli, A.A. Lemonidou, I.A. Vasalos, J. Mol. Catal. A 232 (2005) 29–39.
[19] A. Dejoz, J.M. Lopez Nieto, F. Marquez, M.I. Vazquez, Appl. Catal. A 180 (1999) 83–94.
[20] J.D. Pless, B.B. Bardin, H.-S. Kim, D. Ko, M.T. Smith, R.R. Hammond, P.C. Stair, K.R. Poeppelmeier, J. Catal. 223 (2004) 419–431.
[21] S. Pudar, J. Oxgaard, K. Chenoweth, A.C.T. Van Duin, W.A. Goddard, J. Phys. Chem. C 111 (2007) 16405–16415.
[22] R.K. Grasselli, D.L. Stern, J.G. Tsikoyiannis, Appl. Catal. A 189 (1999) 1–8.
[23] J.G. Tsikoyiannis, D.L. Stern, R.K. Grasselli, J. Catal. 184 (1999) 77–86.
[24] L. Late, W. Thelin, E.A. Blekkan, Appl. Catal. A 262 (2004) 63–68.
[25] R. Le. Mao, S. Melancon, C. Gauthier-Campbell, P. Kletnieks, Catal. Lett. 73 (2–4) (2001) 181–186.
[26] S. Fuchs, L. Leveles, K. Seshan, L. Lefferts, A. Lemonidou, J.A. Lercher, Top. Catal. 15 (2–4) (2001) 169–174.
[27] M. Xu, C. Shi, X. Yang, M.P. Rosynek, J.H. Lunsford, J. Phys. Chem. 96 (15) (1992) 6395–6398.
[28] S.J. Korf, J.A. Roos, N.A. de Bruijn, J.G. van Ommen, J.R.H. Ross, Catal. Today 2 (1988) 535–545.
[29] S.C. Bhumkar, L.L. Lobban, Ind. Eng. Chem. Res. 31 (1992) 1856–1864.
[30] A.A. Lemonidou, A.E. Stambouli, Appl. Catal. A 171 (1998) 325–332.
[31] V.P. Vislovskiy, T.E. Suleimanov, M.Yu. Sinev, Y.P. Tulenin, L.Y. Margolis, V. Cortes Corberan, Catal. Today 61 (2000) 287–293.
[32] K.T. Nguyen, H.H. Kung, J. Catal. 122 (1990) 415–428.
[33] K.-I. Aika, J.H. Lunsford, J. Phys. Chem. 81 (14) (1977) 1393–1398.
[34] K.-I. Aika, J.H. Lunsford, J. Phys. Chem. 82 (16) (1978) 1794–1800.
[35] C.A. Mims, R. Mauti, A.M. Dean, K.D. Rose, J. Phys. Chem. 98 (1994) 13357–13372.
[36] E.V. Kondratenko, M.Yu. Sinev, Appl. Catal. A 325 (2007) 353–361.